ELSEVIER

Ceramics International 25 (1999) 437–445

CERAMICS INTERNATIONAL

# Durability of ceramic filters in the presence of some diesel soot oxidation additives

Laura Montanaro

*Department of Materials Science and Chemical Engineering, Politecnico of Torino, Corso Duca degli Abruzzi, 24 - 10129 Torino, Italy*

Received 20 March 1998; accepted 7 July 1998

**Abstract**

The chemical interactions between sodium (as sulphite), iron and cerium (as oxides), coming from fuel additives, and two ceramic filters, in the working temperature range of a Diesel soot filter, were considered. The filters were a cordierite monolith filter and a wound-fiber filter, made by continuous $Al_2O_3$–$B_2O_3$–$SiO_2$ fibers, respectively. Using X-ray diffraction (XRD) and Hg porosimetry analyses, scanning electron microscopy (SEM) observations and microprobe investigations, the extent of chemical etching, the involved reaction mechanisms and porosity changes were investigated. From the experimental results it was concluded that cerium and iron oxides do not react significantly with these filters, whereas sodium leads to a diffuse etching starting from low working temperatures, by many different mechanisms (solid state diffusion, liquid phase diffusion, evaporation–condensation) as a function of the temperature. However the porosity characteristics of the filters, in terms of total porosity and pore size distribution, were not significantly affected by the described chemical interactions. 

## 1. Introduction

The reduction of Diesel soot emissions in the exhaust system may be performed by trapping particulate by an appropriate filter; soot is periodically burnt for cleaning the filter walls and this filter regeneration step can be started thermically [1–3] or catalitically [4–11].

Particularly during the thermal-activated regenerations, the filters undergo thermo-mechanical constraints and interactions with the chemicals driven by soot, which can induce a reduction in the efficiency and durability of the filters. Previous researches have been concerned with the durability, mainly of the cordierite honeycombs, in the usual operating conditions of a Diesel soot filter [4,12–18].

Specific oxidation catalysts are able to lower the soot ignition temperature during regeneration and consequently to reduce the probability of the high-temperature damaging phenomena; but they could accumulate on the filter and interact with it during its lifetime. Many additives have been proposed, namely noble and transition metal oxides [8,9], metal–organic compounds based on manganese [2], cerium, iron, copper [6], alkaline (sodium, lithium) compounds [10].

This paper widens the previous durability studies to some oxidation catalysts and two commercial ceramic filters, different in design and material.

## 2. Experimental

Two commercial filters were chosen, namely a cordierite ($Mg_2Al_4Si_5O_{18}$) monolith filter (filter A) and a wound-fiber filter, made by continuous $Al_2O_3$–$B_2O_3$–$SiO_2$ fibers (filter B). Their starting characteristics were investigated by XRD, Hg porosimetry, SEM observations and microprobe analyses.

By XRD the filter A is made by indialite, a hexagonal $Mg_2Al_4Si_5O_{18}$ probably containing small amount of iron in solid solution; its starting open porosity ranges between 28 and 34%. The mean pore size was about 10 μm. Filter B is mainly amorphous with traces of $Al_{18}B_4O_{33}$ and its open porosity is 57–62%. The mean pore size was about 23 μm. Both pore size distributions were monomodal. The three chemicals were $Na_2SO_3$, $Fe_2O_3$ (hematite) and $CeO_2$ (cerianite), which represent probable residual products in the soot coming respectively from sodium, iron and cerium-based oxidation catalysts. A carbon black powder was used to simulate soot: it was a microcrystalline graphite having a mean particle size of about 170 nm.

Pellets obtained by uniaxially pressing mixtures (1:1 by weight) of each chemical and powdered filter material were calcined in static air, for 2 h in the range 700 to 1200°C. The calcined materials were then analysed by

0272-8842/99/$20.00 
PII: S0272-8842(98)00051-0

XRD, to investigate new crystalline phase formation. Also temperatures higher than the common operating temperatures of a Diesel soot filter (generally, 250–900°C [1]) were investigated for simulating the hot spot effects during the mean lifetime of a filter.

Small cubes (3 mm in side) of carbon black added respectively with 10 wt% of one chemical were placed on the surface of filter samples and calcined in static air (2 h soaking in the above temperature range; heating and cooling rate of 10°C/min), to simulate the local interaction during soot combustion. The morphology and the phase composition at the contact zone were investigated by SEM and EDS microprobe.

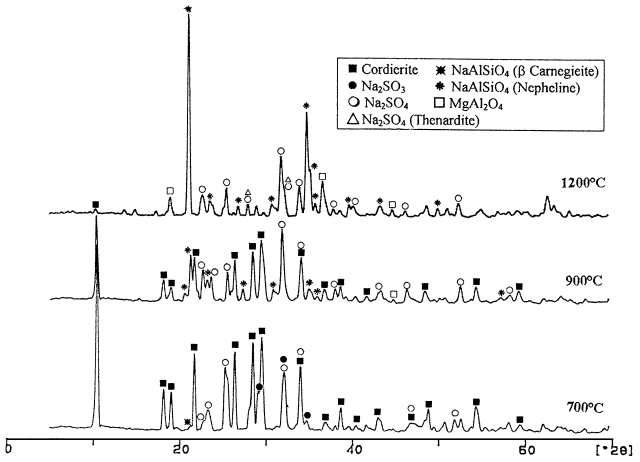


Fig. 1. XRD patterns of the sodium sulphite-filter A mixture calcined at different temperature.

Finally, samples of the filters were immersed in an alcoholic suspensions of carbon black containing respectively 10 wt% of one chemical, to obtain a homogeneous deposit on the filter surface and simulate the accumulation of soot during use. After drying the samples were calcined following the thermal cycles previously described and then characterized by Hg porosimetry to study the changes in porosity.

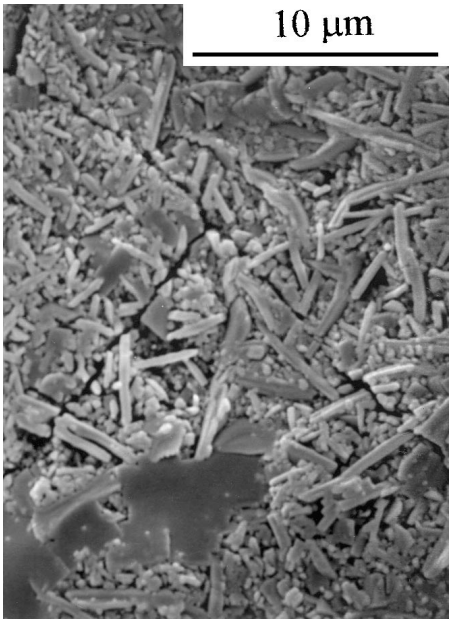


Fig. 3. SEM micrograph of the surface of filter A in contact with the sodium sulphite deposit after calcination at 900°C.

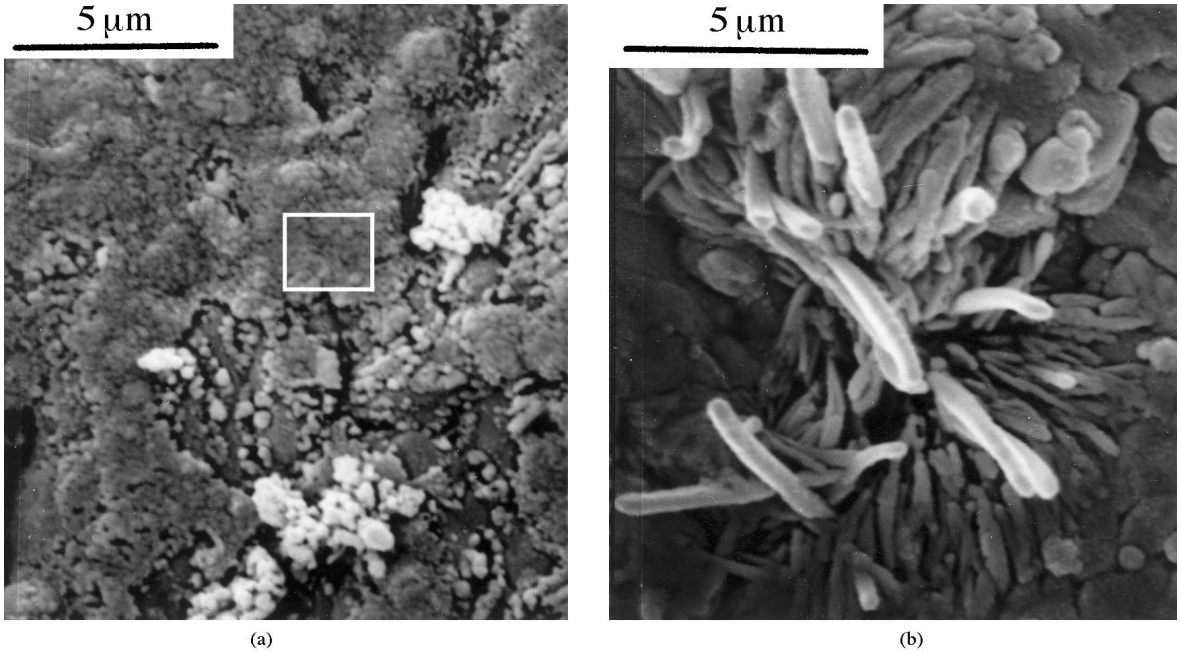


(a) (b)

Fig. 2. SEM micrograph of the surface of filter A in contact with the sodium sulphite deposit after calcination at 700°C: (a) corroded surface; (b) new phase at cordierite grain boundary.

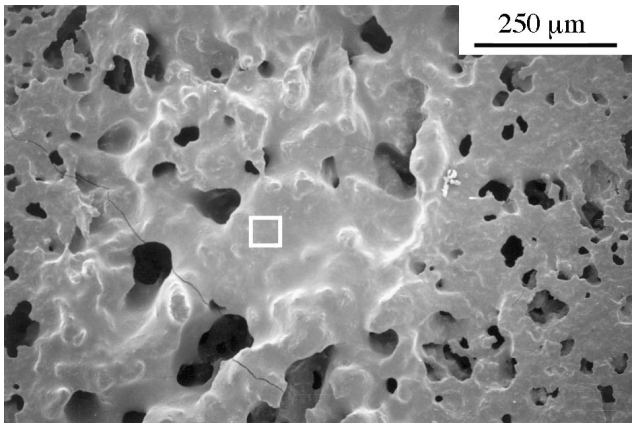


Fig. 4. SEM micrograph of the surface of filter A in contact with the sodium sulphite deposit after calcination at 1200°C: evidence of fused regions.

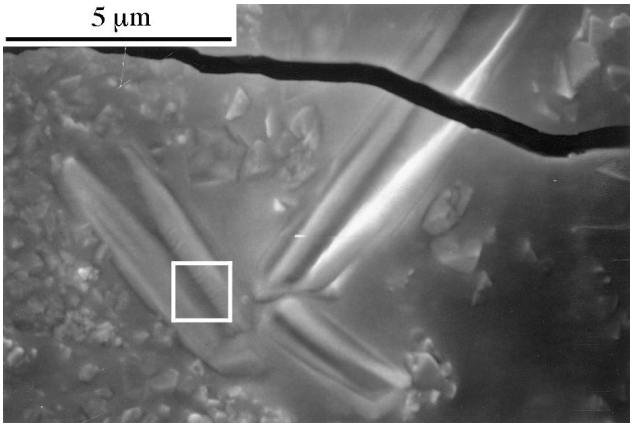


Fig. 5. SEM micrograph of the surface of filter A in contact with the sodium sulphite deposit after calcination at 1200°C: evidence of microcracks and of a new crystalline phase.

## 3. Results and discussion

In Fig. 1 the XRD patterns after some thermal treatments of the sodium sulphite-cordierite mixtures are presented. Starting from 700°C, the sodium compound reacts with cordierite, by a solid state diffusion: a sodium aluminosilicate (β $NaAlSiO_4$, carnegieite) is detected; at the same temperature, sodium sulphite partially transforms in sodium sulphate. At 900°C carnegieite changes into nepheline ($NaAlSiO_4$) which is detected near Mg-Al spinel. Increasing the temperature, all the sodium sulphite changes in sulphate, the new phases remain the same but etching goes on up to the complete consumption of cordierite. These data are in agreement with the previous papers [14–17].

SEM observations confirms that cordierite is etched by the sodium sulphite starting from 700°C: the filter surface is corroded in contact with sodium sulphite deposit and traces of new crystalline phase are present at the cordierite grain boundaries (Fig. 2).

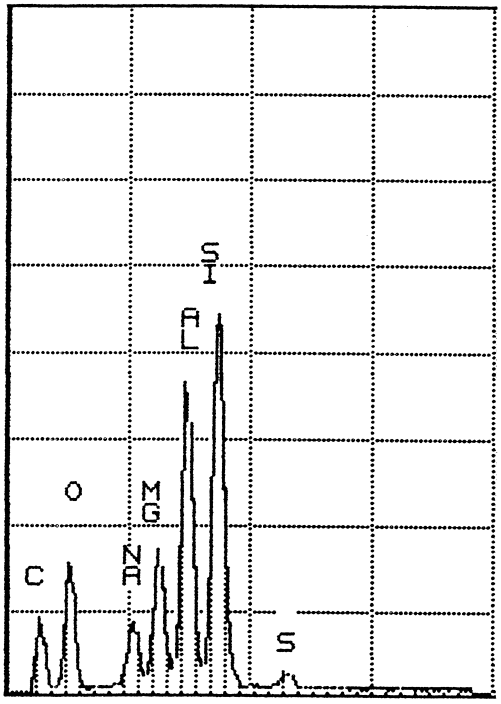


Fig. 6. Microprobe analysis of the surface of filter A in contact with sodium sulphite deposit after calcination at 700°C (performed in the region shown in Fig. 2(a)).

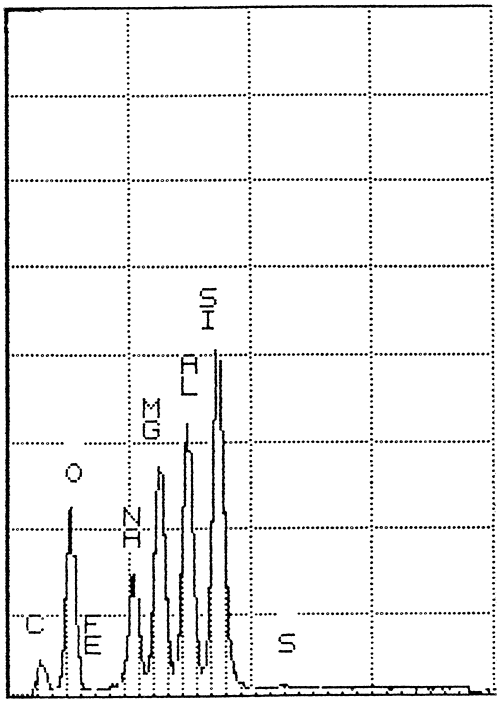


Fig. 7. Microprobe analysis of the surface of filter A in contact with sodium sulphite deposit after calcination at 1000°C (glassy region) (performed in the region shown in Fig. 4).

Etching (surface corrosion, new crystalline phase formation, cracking) is more and more evident increasing the calcination temperature (Fig. 3). Starting from

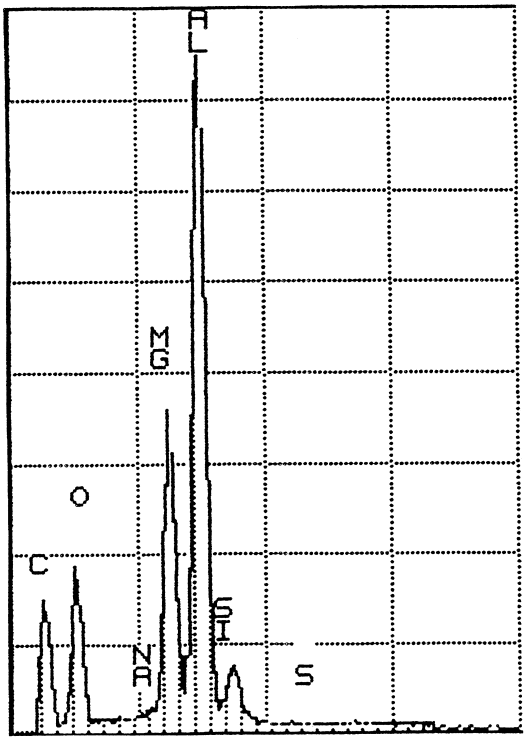


Fig. 8. Microprobe analysis of the surface of filter A in contact with sodium sulphite deposit after calcination at 1200°C (new crystalline phase) (performed in the region shown in Fig. 5).

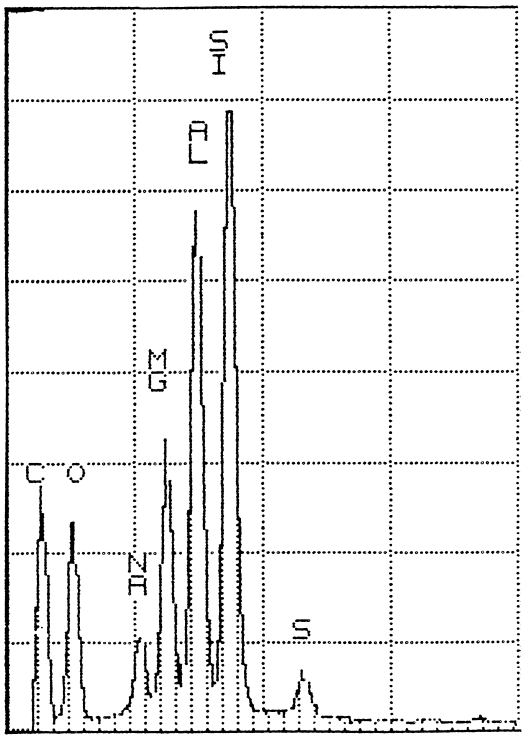


Fig. 9. Microprobe analysis of the surface of filter A far from the contact region with sodium sulphite deposit after calcination at 900°C.

1100°C some fused regions and new crystalline phases were observed; at 1200°C the fused regions are so extended (Fig. 4) to induce a visible local change in porosity; many larger cracks appear and some new crystals grow from the fused regions (Fig. 5).

Considering the data of the microprobe analyses, in the sample treated at 700°C the corroded region in contact with sodium sulphite deposit is enriched in sodium (Fig. 6); starting from 800°C, locally also cordierite stoichiometry changes. Referring to the relative weight percent of the only metal components, evaluated on pure samples, silicon content changes from about 50 wt% of the starting cordierite to more than 66 wt%, aluminium content from about 36 to 21 wt%, magnesium from less than 13 to about 8 wt%. This is in agreement with the formation of a sodium aluminosilicate and Mg–Al spinel, yielded by the cordierite etching and detected by XRD.

At higher temperatures, in the fused regions observed by SEM, a high sodium content was detected (5–13 wt%,Fig. 7). The elongated crystals grown from the fused regions presented Mg and Al weigth percentages similar to those of Mg–Al spinel (Fig. 8).

Over 1000°C, in parts of the samples far from the deposit, an increasing amount of sodium was detected as a function of the calcination temperature (Fig. 9): its amount can reach 6 wt%.

Coupling SEM observations and microprobe analyses, some hypotheses on the diffusion mechanisms may be done. There is evidence that from 1000°C, due to the formation of low melting point (lower than 1000°C) eutectics [19] and to the sodium sulphate melting [20], a liquid phase diffusion mechanism becomes active, besides the solid state diffusion. In the same temperature range, a grain boundary diffusion of molten $Na_2SO_4$ in a sintered mullite has been already shown [21]. This mechanism allows the sodium transport by liquid phase infiltration in the porosity of the cordierite filter walls: in this way, regions far from the local contact between the filter and the sodium compound can undergo alterations.

From about 1100°C, a third mechanism should be present, namely the evaporation–condensation diffusion of sodium oxide, as shown by the microprobe analyses, which can involve more and more large areas.

Microcracks formation should be explained by the appearance of new, amorphous and/or crystalline phases, having different thermal expansion coefficients than that of cordierite. For instance, whereas for pure cordierite $\alpha$ is about $1.7–3.7\times10^{-6}/°C$, the values for Mg–Al spinel and for nepheline are $5.0\times10^{-6}/°C$ and about $13.0\times10^{-6}/°C$, respectively. However, the total porosity and pore size distribution of this filter are not significantly affected by these microstructural modifications, as shown by Hg porosimetry (Fig. 10).

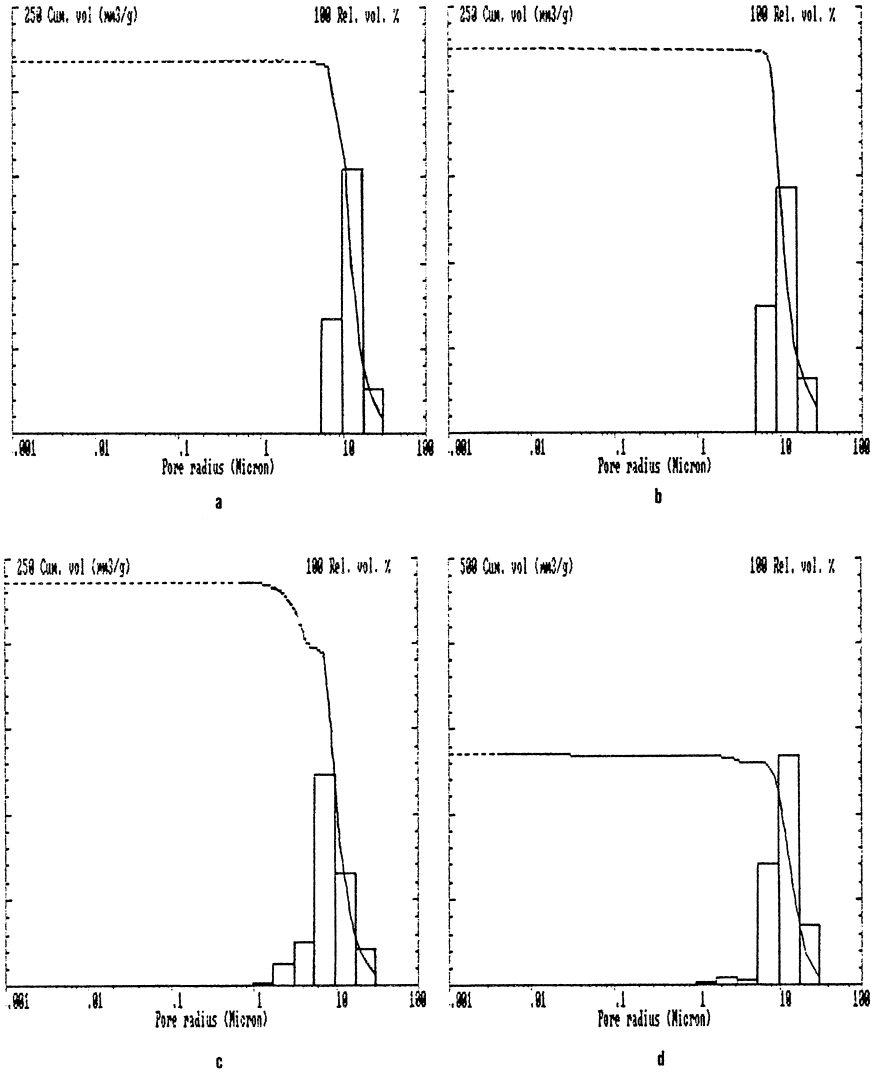


Fig. 10. Pore size distribution of filter A as a function of calcination temperature in the presence of sodium sulphite: (a) as-received filter; (b) calcined at 800°C; (c) calcined at 1000°C; (d) calcined at 1200°C.

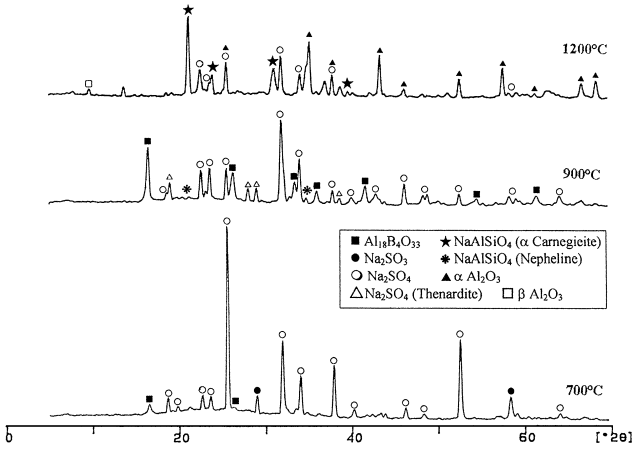


Fig. 11. XRD patterns of the sodium sulphite-filter B mixture calcined at different temperatures.

In the case of filter B, during calcination, independently of any reaction with sodium compound, the spontaneous fiber crystallization to yield $Al_{18}B_4O_{33}$ was detected by XRD (Fig. 11). In addition, at 900°C, nepheline is yielded by solid-state reaction with sodium and sodium sulphite is already completely transformed in sulphate. Starting from 1000°C, α alumina appears near sodium aluminosilicate; at 1200°C α carnegieite (α $NaAlSiO_4$) and α alumina are strongly prevalent, traces of β alumina (sodium doped alumina) were detected whereas $Al_{18}B_4O_{33}$ completely disappeared.

From 900°C, surface corrosion near the deposit and new crystals growing from fibers were shown by SEM (Fig. 12). At higher temperature, the liquid phase diffusion makes the interaction more significant: many fibers stick together and hexagonal and acicular crystals can be clearly observed (Fig. 13).

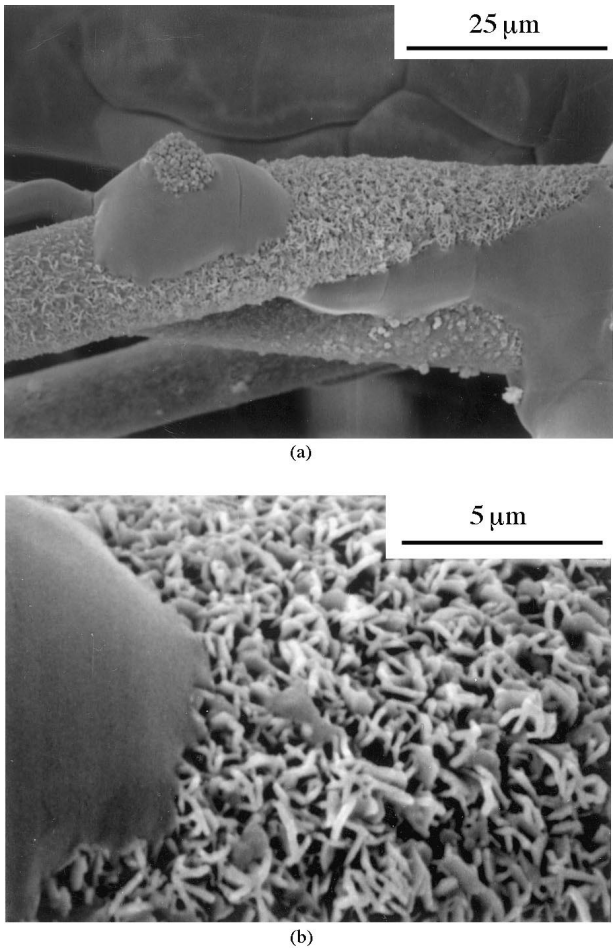


Fig. 12. SEM micrograph of the surface of filter B in contact with the sodium sulphite deposit after calcination at 900°C: (a) general view; (b) detail of the new crystalline phase.

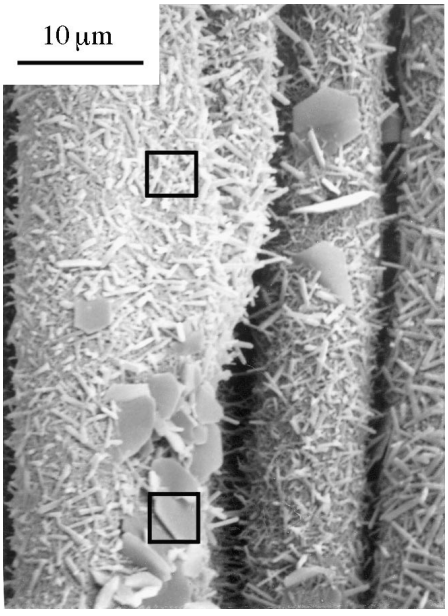


Fig. 13. SEM micrograph of the surface of filter B in contact with the sodium sulphite deposit after calcination at 1100°C.

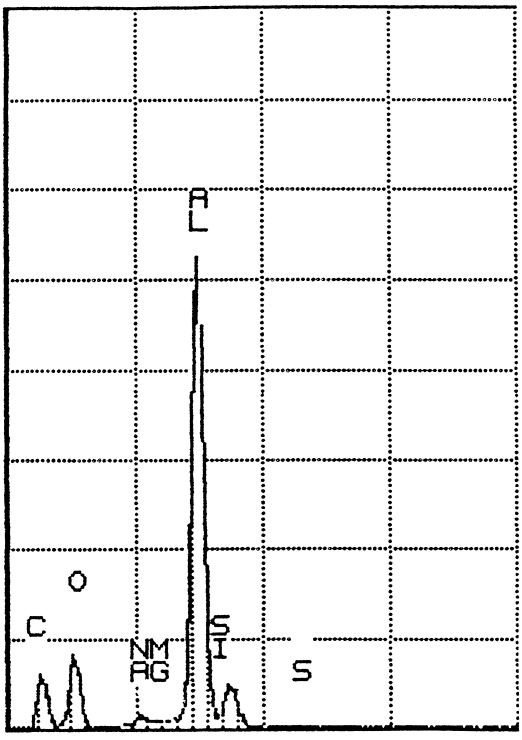


Fig. 14. Microprobe analysis of the surface of filter B in contact with sodium sulphite deposit after calcination at 1200°C (new hexagonal crystals) (performed in the region shown in Fig. 13).

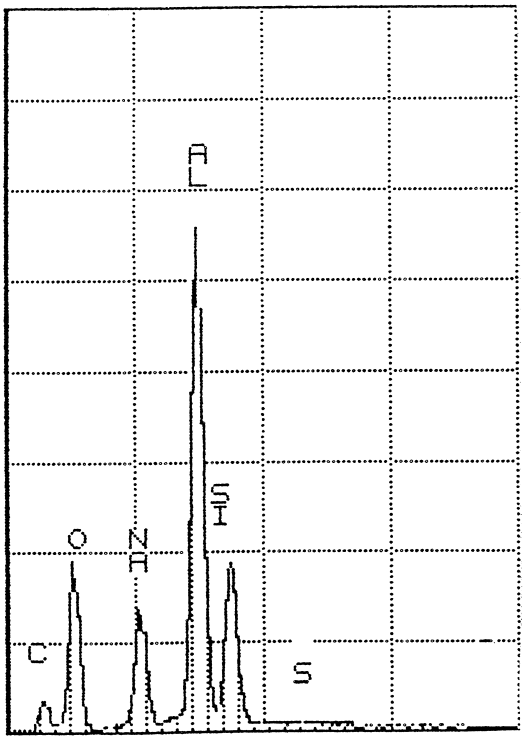


Fig. 15. Microprobe analysis of the surface of filter B in contact with sodium sulphite deposit after calcination at 1200°C (new acicular crystals) (performed in the region shown in Fig. 13).

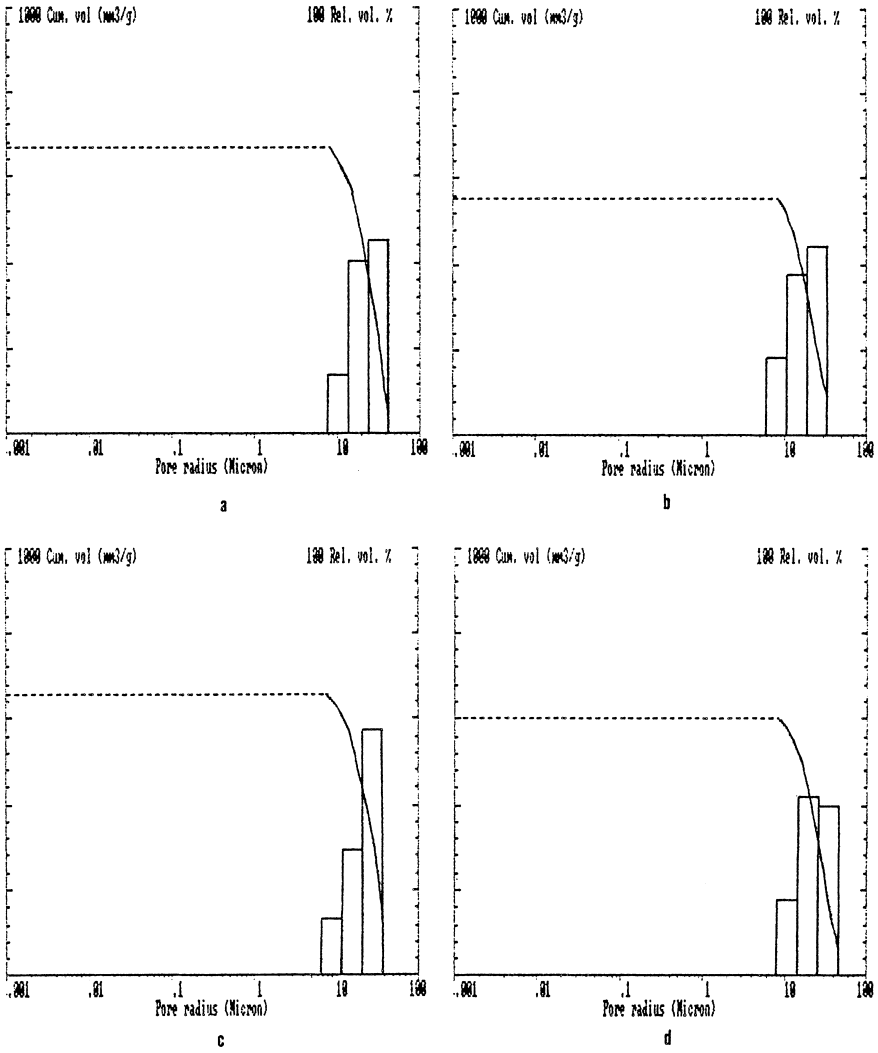


Fig. 16. Pore size distribution of filter B as a function of calcination temperature in the presence of sodium sulphite: (a) as-received filter; (b) calcined at 800°C; (c) calcined at 1000°C; (d) calcined at 1200°C.

These two crystalline species were respectively identified to be α alumina (Fig. 14) and a sodium aluminosilicate (Fig. 15) by microprobe analyses, in agreement with XRD data. Also for the sample B, at temperatures higher than 1000°C, high sodium amounts were detected far from the sodium sulphite deposit, due to evaporation-condensation. Therefore, it can be reasonably supposed that the three etching mechanisms, above discussed for filter A, are active, as a function of the calcination temperature, also in this case.

All the microstructural changes observed in sample B could lead to a reduction in the mechanical response, but they did not produce a detectable variation of the porosity characteristics of this filter (Fig. 16).

All the above results assess the high reactivity of sodium compounds versus aluminosilicate materials, even if in this case sodium sulphite and sulphate are the reactants involved. In fact, as demonstrated in a study on mullite corrosion [21], at 1000°C $Na_2SO_4$ decomposes in $Na_2O_{(s,l)}$ to a lower extent than $Na_2CO_3$, used in previous investigations on cordierite durability [14,16,17]: thus, even if a less active sodium compound was used, a strong etching was observed.

On the other hand, in all the investigated temperature range, cerium oxide does not react with the ceramic filters (Fig. 17). No evidence of microstructural changes (Fig. 18) or of a solid state diffusion, even by microprobe investigations, was found.

In the case of the iron additive, limited local interactions between iron oxide and filters A and B were observed, starting from 1100°C, in agreement with previous investigation [18]: however, it was not possible to identify any new phase (Fig. 19) or significant glassy regions; the solid state solubilization of iron in the cordierite lattice of filter A can be reasonably supposed but no experimental evidence was found. Consequently, also the porosity characteristics of the filters were not affected by the presence of these compounds.

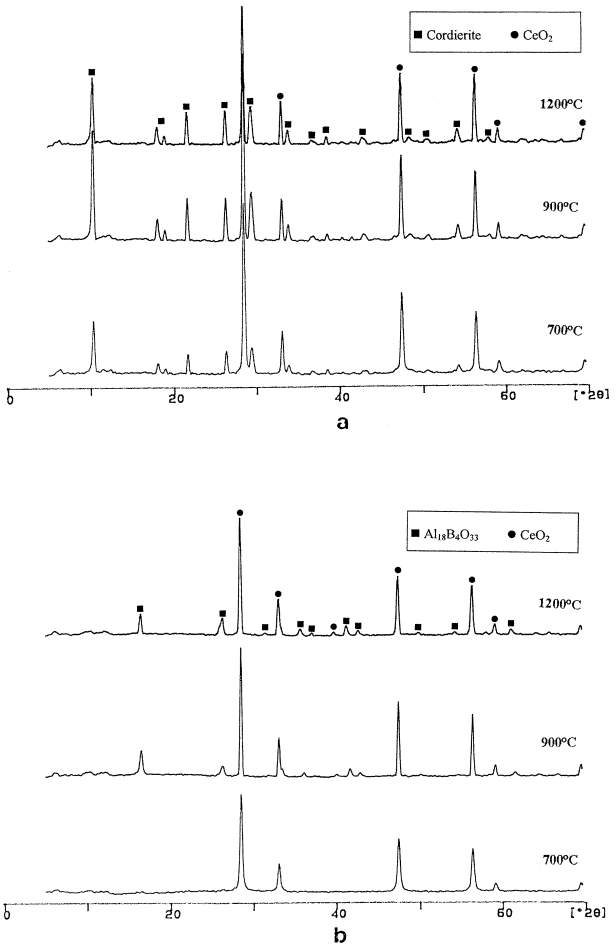


Fig. 17. XRD patterns of the cerium oxide-filter A (a) and filter B (b) mixtures calcined at different temperature.

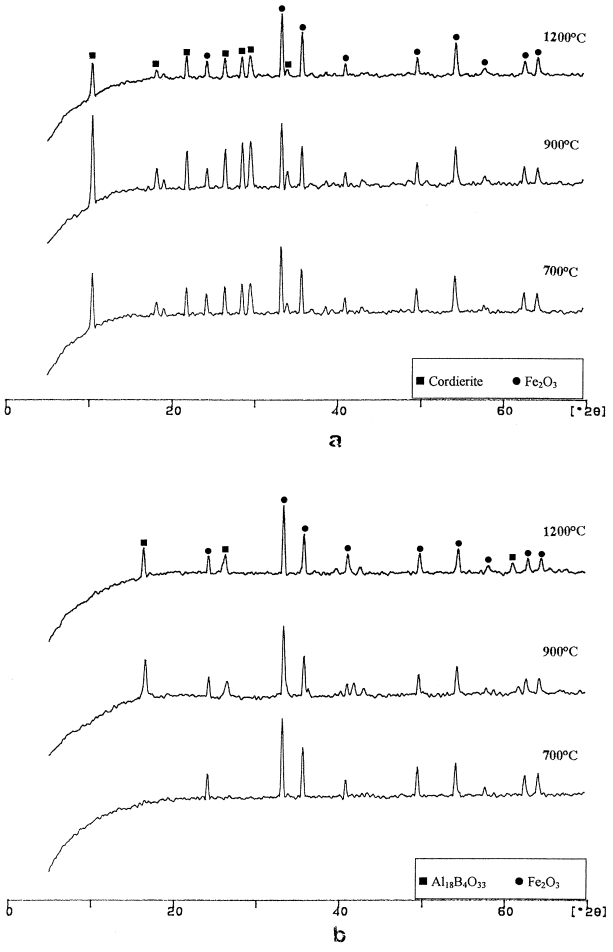


Fig. 19. XRD patterns of the iron oxide-filter A (a) and filter B (b) mixtures calcined at different temperature.

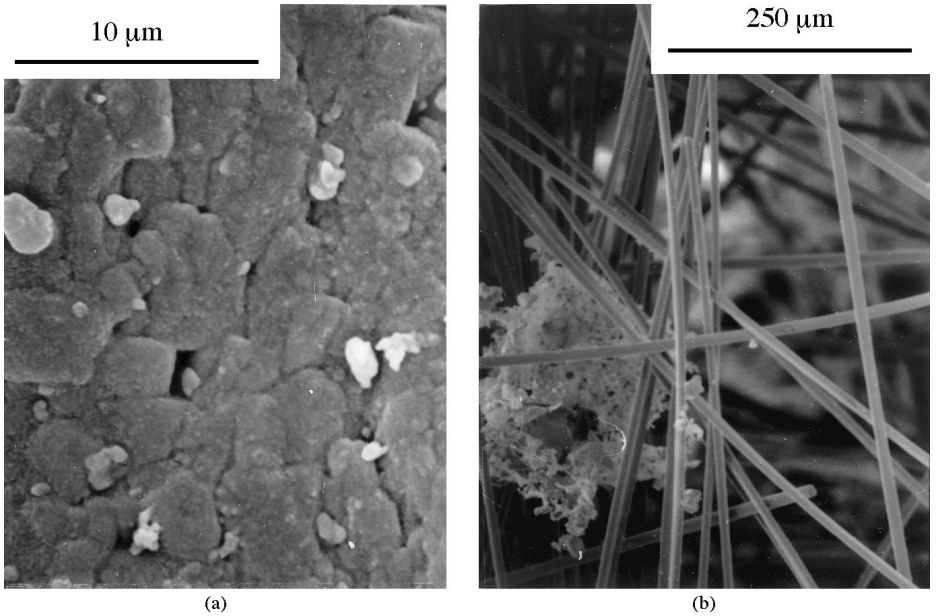


Fig. 18. SEM micrograph of the surface of filter A (a) and filter B (b) in contact with the cerium oxide deposit after calcination at 1100°C.

## 4. Conclusions

The following conclusions can be drawn based on the above results:

1. the residual products of a sodium-based pollutant are likely to react with the ceramic materials of the filters A and B, starting from very low temperatures (700–800°C), by many different mechanisms (solid state diffusion, liquid phase diffusion, evaporation–condensation) as a function of the calcination temperature. As a consequence of the microstructural and compositional changes (new crystalline and glassy phase formation, microcracking, sticking of fibers), near to spontaneous phenomena, such as the crystallization of fibers in filter B, it is reasonably to predict a decrease of the mechanical performances of both ceramic filters. Nevertheless, considering the results of the porosimetric analyses, the filtration efficiency seems to be unchanged;
2. cerium oxide does not react with the considered filters, even in the higher temperature range;
3. also iron oxide does not give rise to detectable interaction with these filters, even if, in the case of filter A, iron should be solubilized in the $Mg_2Al_4Si_5O_{18}$ lattice, to give more iron-substitued indialites.

## References


[1] G.M. Cornetti, P.P. Messori, C. Operti, Development of a ceramic particulate trap for urban buses, Trans. of ASME, Journal of Eng. for Gas Turbines and Power 111 (1989) 398–403.

[2] M. Arai, S. Miyashita, K. Sato, Development and selection of Diesel particulate trap regeneration system, SAE paper 870012, Diesel Exhaust Aftertreatment, Society of Automotive Engineers Inc., Warrendale, PA, USA, 1987, pp. 27–36.

[3] Y. Goto, T. Sato, M. Hayashida, Study on regeneration of Diesel particle trapper by electrical self-heating type filter, SAE paper 920140, Diesel Exhaust Aftertreatment, Society of Automotive Engineers Inc., Warrendale, PA, USA, 1992, pp. 13–23.

[4] K. Pattas, P. Samaras, D. Sherwood, K. Umehara, C. Cantiani, O.A. Chariol, P. Barthe, J. Lemaire, Cordierite filter durability with cerium fuel additive: 100000 km of revenue service in Athens, SAE paper 920363, Diesel Exhaust Aftertreatment, Society of Automotive Engineers Inc., Warrendale, PA, USA, 1992, pp. 289–301.

[5] V.D.N. Rao, H.A. Cokanek, R.W. Horrocks, Diesel particulate control system for Ford 1.8 L Sierra Turbo-Diesel to meet 1997-2003 particulate standards, SAE paper 940458, Diesel Exhaust Aftertreatment, Society of Automotive Engineers Inc., Warrendale, PA, USA, 1994, pp. 197–212.

[6] G. Lepperhoff, H. Luders, P. Barthe, J. Lemaire, Quasi-continuous particle trap regeneration by cerium-additives, SAE paper 950369, Diesel Exhaust Aftertreatment, Society of Automotive Engineers Inc., Warrendale, PA, USA, 1995, pp. 91–102.

[7] G. Lepperhoff, J. Widdershoven, G. Lütkemeyer, I. Hedin, An exhaust gas aftertreatment system to reduce particulates for full-size passenger cars, SAE paper 880003, Diesel Exhaust Aftertreatment, Society of Automotive Engineers Inc., Warrendale, PA, USA, 1988, pp. 9–16.

[8] A.F. Ahlstrom, C.U.I. Obenbrand, Catalytic combustion of soot deposits for Diesel engines, Applied Catalysis 60 (1990) 143–156.

[9] A.F. Ahlstrom, C.U.I. Obenbrand, Catalytic combustion of soot deposits for Diesel engines on mixed oxides of vanadium pentoxide and cupric oxide, Applied Catalysis 60 (1990) 157–172.

[10] B. Krutzsch, G. Wenninger, Effect of sodium and lithium based fuel additives on the regeneration efficiency of Diesel particulate filter, SAE paper 922188, Diesel Exhaust Aftertreatment, Society of Automotive Engineers Inc., Warrendale, PA, USA, 1992, pp. 1–14.

[11] K. Pattas, Z. Samaras, A. Roumbos, J. Lemaire, W. Mustel, P. Rouveirolles, Regeneration of DPF at low temperatures with the use of a cerium based fuel additive, SAE paper 960135, Diesel Exhaust Aftertreatment, Society of Automotive Engineers Inc., Warrendale, PA, USA, 1996, pp. 71–83.

[12] S.T. Gulati, J.C. Summers, D.G. Linden, J.J. White, Improvements in converter durability and activity via catalyst formulation, SAE paper 890796, Diesel Exhaust Aftertreatment, Society of Automotive Engineers Inc., Warrendale, PA, USA, 1989, pp. 1–8.

[13] S.T. Gulati, Long-term durability of ceramic honeycombs for automotive emissions control, SAE paper 850130, Diesel Exhaust Aftertreatment, Society of Automotive Engineers Inc., Warrendale, PA, USA, 1985, pp. 1–16.

[14] A. Negro, L. Montanaro, P.P. Demaestri, A. Giachello, A. Bachiorrini, Interaction between some oxides and cordierite, Journal of the European Ceramic Society 12 (1993) 493–498.

[15] P. Scardi, N. Sartori, A. Giachello, P.P. Demaestri, F. Branda, Influence of calcium oxide and sodium oxide on the microstructure of cordierite catalyst supports, Ceramics International 19 (1993) 105–111.

[16] L. Montanaro, A. Bachiorrini, A. Negro, Deterioration of cordierite honeycomb structure for Diesel emissions control, Journal of the European Ceramic Society 13 (1994) 129–134.

[17] L. Montanaro, A. Bachiorrini, Influence of some pollutants on the durability of cordierite filters for Diesel cars, Ceramics International 20 (1994) 169–174.

[18] P. Scardi, N. Sartori, A. Giachello, P.P. Demaestri, F. Branda, Thermal stability of cordierite catalyst supports contaminated by $Fe_2O_3$, ZnO and $V_2O_5$, Journal of the European Ceramic Society 13 (1994) 275–282.

[19] E.M. Levin, C.R. Robbins, H.F. McMurdie (Eds.), Phase Diagrams for Ceramists, The American Ceramic Society, Columbus, OH, 1964, p. 181.

[20] H.G. Wiedemann, W. Smykatz-Kloss, W. Eysel, DTA and high temperature XRay investigations on natural and synthetic thenardites $Na_2SO_4$, in: W. Hemminger (Ed.), Thermal Analysis, vol. 2, Birkhauser Verlag, Basel, 1980, pp. 347–352.

[21] N.S. Jacobson, K.N. Lee, T. Yoshio, Corrosion of mullite by molten salts, J. American Ceramic Society 79 (8) (1996) 2161–2167.